

Neutrino-deuteron reactions at solar neutrino energies

S. Nakamura¹, T. Sato^{1,2}, S. Ando², T.-S. Park², F. Myhrer², V. Gudkov²
and
K. Kubodera²

¹*Department of Physics, Osaka University, Toyonaka, Osaka 560-0043, Japan*

²*Department of Physics and Astronomy, University of South Carolina,
Columbia, SC 29208, USA*

February 9, 2020

Abstract

In interpreting the SNO experiments, very accurate estimates of the νd reaction cross sections are of great importance. We improve the previous estimates of our group by updating some of its inputs and by taking into account the results of a recent effective-field-theoretical calculation. The new cross sections are slightly ($\sim 1\%$) larger than the previously reported values. We present arguments that lead to the conclusion that it is reasonable to assign 1% uncertainty to the νd cross sections reported here.

PACS : 25.30.Pt, 25.10.+s, 26.65.+t, 95.30.Cq

Key words : neutrino deuteron reaction, solar neutrino, exchange current , effective field theory, radiative corrections

1. Introduction

The establishment of the Sudbury Neutrino Observatory (SNO) [1, 2] has motivated intensive theoretical effort to make reliable estimates of the neutrino-deuteron reaction cross sections [3, 4, 5]. One of the primary experiments at SNO is the measurement of the solar neutrino flux. By observing the charged-current (CC) reaction, $\nu_e d \rightarrow e^- pp$, one can determine the flux, $\phi(\nu_e)$, of the solar electron-neutrinos while, by monitoring the neutral-current (NC) reaction, $\nu_x d \rightarrow \nu_x pn$ ($x = e, \mu$ or τ), one can determine $\phi(\nu)$, the total flux of the solar neutrinos of any flavors. These features make SNO a unique facility for studying neutrino oscillations. SNO is also capable of monitoring the yield of the neutrino-electron elastic scattering (ES), $\nu_e e \rightarrow \nu_e e$, which also carries information on neutrino oscillations. The first report from SNO [2] was concerned with the measurements of the CC and ES processes. By combining the SNO data on the CC reaction with the Super-Kamiokande data on ES [6],¹ strong evidence for ν_e oscillations has been obtained [2]. It is to be noted that the sharpness of this important conclusion depends on the precision of theoretical estimates for the νd -reaction cross sections. In the present communication we wish to describe our attempt to improve the existing estimates.

¹The SNO data on ES is consistent with the Super-K data [6] but the latter has higher statistics.

We first give a brief survey of the theoretical estimates of the νd -reaction cross section that were used in the analysis in [2].² A highly successful method for describing nuclear responses to electroweak probes is to consider one-body impulse approximation (IA) terms and two-body exchange-current (EXC) terms acting on non-relativistic nuclear wave functions, with the EXC contributions derived from one-boson exchange diagrams [7]. We refer to this method as the standard nuclear physics approach (SNPA)[8].³ The most elaborate calculation of the νd cross sections based on SNPA has been done by Nakamura *et al.* (NSGK) [4]. Since the νd reactions in the solar neutrino energy ($E_\nu \leq 20$ MeV) is dominated by the contribution of the space component, \mathbf{A} , of the axial current (A_μ), the theoretical precision of $\sigma_{\nu d}$ is controlled essentially by the accuracy with which one can calculate the nuclear matrix element of \mathbf{A} . Let us decompose \mathbf{A} as $\mathbf{A} = \mathbf{A}_{\text{IA}} + \mathbf{A}_{\text{EXC}}$, where \mathbf{A}_{IA} and \mathbf{A}_{EXC} are the IA and EXC contributions, respectively. Since \mathbf{A}_{IA} is well known, the theoretical uncertainty is confined to \mathbf{A}_{EXC} . Now, among the various terms contributing to \mathbf{A}_{EXC} , the Δ -excitation current (\mathbf{A}_Δ) gives the most important contribution [9], and \mathbf{A}_Δ involves the coupling constants for the $A_\mu N \Delta$ vertex, the $\pi(\rho) N \Delta$ vertex and the vertex form factors. Although each of the coupling constants can be reasonably estimated by using the quark model, their empirical values are not available separately. Only the whole of the strength of the Δ -excitation current can be tested with electroweak processes in a few nucleon system. NSGK therefore considered two methods for controlling the strength of the Δ -excitation current. In one method, by exploiting the fact that the Δ -excitation current features in the $np \rightarrow \gamma d$ amplitude as well, the strength of it is determined to reproduce the $np \rightarrow \gamma d$ cross section. The second method uses the tritium β decay rate, Γ_t^β , and as in Refs.[9, 10], the strength of the Δ -excitation current is adjusted to reproduce the well known experimental value of Γ_t^β . The first method was found to give $\sigma_{\nu d}$ about 3% larger than the second method, and NSGK adopted this 3% difference as a measure of uncertainty in their calculation based on SNPA.

Apart from SNPA, a new approach based on effective field theory (EFT) has been scoring great success in describing low-energy phenomena in few-nucleon systems [11, 12, 13]. Butler *et al.* (BCK) [5] applied EFT to the νd reactions, using the regularization scheme called the power divergence subtraction (PDS) [14]. Their results agree with those of NSGK in the following sense. The EFT Lagrangian used by BCK involves one unknown low-energy constant (LEC), denoted by L_{1A} , which represents the strength of A_μ -four-nucleon contact coupling. BCK adjusted L_{1A} to optimize fit to the $\sigma_{\nu d}$ of NSGK and found that, after this optimization, the results of the EFT and SNPA calculations agree with each other within 1% over the entire solar- ν energy region. Furthermore, the best-fit value of L_{1A} turned out to be consistent with what one would expect from the “naturalness” argument [5]. The fact that the results of an *ab initio* calculation (modulo one free parameter) based on EFT are completely consistent with those of SNPA may be taken as evidence for the basic soundness of SNPA.

Having given a brief survey of the existing theoretical estimates of $\sigma_{\nu d}$, we now describe several points that need to be addressed for improving the estimates. We first note that, as pointed out by Beacom and Parke [15], the value of the axial coupling constant, g_A , used in NSGK is not the most updated one. This obvious deficiency needs to be remedied. Secondly, in their treatment of \mathbf{A}_{EXC} , NSGK left out some sub-dominant diagrams, and therefore it is worthwhile to examine the consequences of using the full set of relevant Feynman diagrams [10]. Furthermore, NSGK adopted as their *standard run* the case in which the strength of the Δ -excitation current was adjusted to

² In what follows, $\sigma_{\nu d}^{CC}$ and $\sigma_{\nu d}^{NC}$ stand for the total cross sections (in the laboratory frame) for the CC and NC reactions, respectively; in referring to $\sigma_{\nu d}^{CC}$ and $\sigma_{\nu d}^{NC}$ collectively, we use the generic symbol, $\sigma_{\nu d}$. The incident neutrino energy in the lab-frame will be denoted by E_ν .

³ This approach was called the phenomenological Lagrangian approach (PhLA) in [4].

reproduce the measured $np \rightarrow \gamma d$ rate. However, the $np \rightarrow d\gamma$ reaction governed by the vector current cannot be considered as a better constraint than Γ_t^β for monitoring the effective strength of $g(A_\mu N\Delta)$ relevant to the axial-vector transition. In the present work, therefore, we adopt as our standard choice the case in which \mathbf{A}_{EXC} is controlled by Γ_t^β . Thirdly, at the level of precision in question, radiative corrections become relevant [15, 16, 17]. In this communication, however, we do not address radiative corrections *per se* and simply refer to the literature on this issue [15, 17]. A related problem is what value should be used for the weak coupling constant. One possibility is to use the standard Fermi constant, G_F , which has been derived from μ -decay and hence does not contain any hadron-related radiative corrections. Another possibility is to employ an effective coupling constant (denoted by G_F') that includes the so-called inner radiative corrections for nuclear β -decay. NSGK adopted the first choice. However, since the inner corrections are established reasonably well, it seems more natural to use G_F' instead of G_F . We therefore adopt here G_F' as the weak coupling constant (see below for more detail). An additional point that warrants a further study is the stability of the calculated value of $\sigma_{\nu d}$ against different choices of the NN interactions. NSGK investigated this aspect for a rather wide variety of the modern high-quality NN interactions [18, 19] and found the stability of $\sigma_{\nu d}$ at the 0.5% level. The interactions considered in NSGK, however, are all local potentials and have similar values of the deuteron D -state probability, P_D . Since the CD-Bonn potential [20] has a somewhat smaller value of P_D than the other modern high-quality NN potentials, we study here whether the stability persists with the use of the CD-Bonn potential.

Besides these improvements within the framework of SNPA, we present here a new comparison between SNPA and EFT. Park *et al.* [21, 22, 23] have developed an EFT approach wherein the electroweak transition operators are derived with a cut-off scheme EFT (à la Weinberg [11]) and the initial and final wave functions are obtained with the use of the high-quality phenomenological nuclear interactions. For convenience, we refer to this approach as EFT*. EFT* applied to the Gamow-Teller transitions contains one unknown LEC denoted by \hat{d}_R , which plays a role similar to L_{1A} in BCK. In EFT*, however, one can determine \hat{d}_R *directly* from Γ_t^β [23]. This allows a parameter-free EFT calculation of $\sigma_{\nu d}$, and very recently Ando *et al.* have carried out this type of calculation [24]. We present a comparison between our new results based on SNPA and those based on EFT*, and we argue that good agreement between them renders further support for the robustness of $\sigma_{\nu d}$ obtained in SNPA. It will be seen that the new values of $\sigma_{\nu d}$ are close to those given in NSGK, but that a significant improvement in error estimates has been achieved.

2. Calculation and numerical results

The calculational framework used here is the same as in NSGK except for the following points. For the weak coupling constant, instead of $G_F = 1.16637 \times 10^{-5} \text{ GeV}^{-2}$ employed in NSGK, we adopt $G_F' = 1.1803 \times 10^{-5} \text{ GeV}^{-2}$ obtained from $0^+ \rightarrow 0^+$ nuclear β -decays [25].⁴ Thus G_F in Eq.(7) and Eq.(8) in NSGK should be replaced by G_F' . G_F' subsumes the bulk of the *inner* radiative corrections.⁵ The Cabibbo factor in Eq.(7) of NSGK is taken to be $\cos\theta_C = 0.9740$. For g_A , we adopt the current standard value, $g_A=1.267$, instead of $g_A=1.254$ used in NSGK. In addition, as the axial-vector mass, we choose the value given in the latest analysis [26]. To implement these

⁴ The relation between G_F' and the quantities used in [25] is: $G_F'^2 = (G_V/V_{ud})^2(1 + \Delta_R^V)$, where V_{ud} is the K-M matrix element, and Δ_R^V is the nucleus-independent radiative correction.

⁵ To be precise, the inner corrections for the CC and NC reactions may differ but the difference reported in the literature [17] is comparable to the estimated uncertainty of our present calculation (see below).

changes, we only need replace Eq.(24) in [4] with

$$f_A(q_\mu^2) = -1.267 G_A(q_\mu^2), \quad (1)$$

where

$$G_A(q_\mu^2) = \left(1 - \frac{q_\mu^2}{1.04 \text{ GeV}^2}\right)^{-2}. \quad (2)$$

The change in $G_A(q_\mu^2)$ is in fact not consequential for $\sigma_{\nu d}$ in the solar- ν energy region. We employ here the \mathbf{A}_{EXC} of Schiavilla *et al.* [10], which reproduces the experimental value of Γ_t^β . It consists of the π -pair current (denoted by πS), ρ -pair current (ρS), π -exchange Δ -excitation current ($\Delta\pi$), ρ -exchange Δ -excitation current ($\Delta\rho$) and $\pi\rho$ -exchange current ($\pi\rho$). The explicit expressions of these currents are given in the Appendix. All the other ingredients used in the present calculation are the same as those used in the “*standard run*” in NSGK. In particular, the AV18 potential [18] is used to generate the initial and final two-nucleon states. The above-described set of input defines a bench mark case in our new calculation, and we shall refer to it as the *standard case*.⁶ Other cases, which we consider for checking the stability of the results of the *standard case*, will be specified explicitly as needed.

For the *standard case* we have calculated the total cross sections and differential cross sections (up to $E_\nu = 170$ MeV) for the four reactions:

$$\nu_e + d \rightarrow e^- + p + p \quad (\text{CC}) \quad (3)$$

$$\nu_x + d \rightarrow \nu_x + n + p \quad (\text{NC}) \quad (4)$$

$$\bar{\nu}_e + d \rightarrow e^+ + n + n \quad (\bar{\nu}\text{-CC}) \quad (5)$$

$$\bar{\nu}_x + d \rightarrow \bar{\nu}_x + n + p \quad (\bar{\nu}\text{-NC}) \quad (6)$$

In this article we concentrate on the quantities directly relevant to the SNO solar neutrino experiments and limit ourselves to the neutrino reactions (CC and NC) for $E_\nu \leq 20$ MeV.⁷ The $\sigma_{\nu d}$ corresponding to the *standard case* is shown in Table 1 as a function of E_ν .⁸ The results given in Table 1 should supersede the corresponding results in NSGK. In the following we discuss comparison between the new and old estimates of $\sigma_{\nu d}$ as well as error estimates for the new calculation.

For clarity, when necessary, the total cross sections corresponding to the *standard case* of the present work are denoted by $\sigma_{\nu d}(\text{Netal})$, $\sigma_{\nu d}^{CC}(\text{Netal})$ and $\sigma_{\nu d}^{NC}(\text{Netal})$; those corresponding to the *standard run* in NSGK are denoted by $\sigma_{\nu d}(\text{NSGK})$, $\sigma_{\nu d}^{CC}(\text{NSGK})$ and $\sigma_{\nu d}^{NC}(\text{NSGK})$. The ratio of $\sigma_{\nu d}^{CC}(\text{Netal})$ to $\sigma_{\nu d}^{CC}(\text{NSGK})$ is given for several representative values of E_ν in the first column of Table 2. Similar information for $\sigma_{\nu d}^{NC}$ is given in the second column. As the table indicates, $\sigma_{\nu d}^{CC}(\text{Netal})$ is slightly larger than $\sigma_{\nu d}^{CC}(\text{NSGK})$; the difference is $\sim 1.3\%$ for $E_\nu \sim 5$ MeV, $\sim 0.8\%$ for $E_\nu \sim 10$ MeV, and $\sim 0.4\%$ for $E_\nu \sim 20$ MeV. A similar tendency is seen for $\sigma_{\nu d}^{NC}$ as well. The origins of the difference between $\sigma_{\nu d}(\text{Netal})$ and $\sigma_{\nu d}(\text{NSGK})$ will be analyzed below.

Changing the weak coupling constant from G_F to G'_F scales $\sigma_{\nu d}$ by an overall factor of $(G'_F/G_F)^2 \sim 1.02$. The effect of changing the value of g_A can also be well simulated by an overall factor, since the νd reaction at low energies is dominated by the Gamow-Teller transition

⁶ The *standard case* here should not be confused with the *standard run* in NSGK.

⁷ A fuller account of the present calculation will be published elsewhere. The full presentation of the numerical results of the present work can be found at the web site: <<http://nuc003.psc.sc.edu/~kubodera/NU-D-NSGK>>.

⁸ The numerical precision of our computation of the cross sections is 0.1% for $E_\nu \leq 20$ MeV.

and hence $\sigma_{\nu d}$ is essentially proportional to g_A^2 . Thus the change of g_A from $g_A = 1.254$ to $g_A = 1.267$ enhances $\sigma_{\nu d}$ in the low-energy region by another factor of $(1.267/1.254)^2 \sim 1.02$.

In discussing the consequences of the change in \mathbf{A}_{EXC} , it is convenient to introduce the terms, Models I and II. As described earlier, our *standard case* uses the \mathbf{A}_{EXC} given in [10]. We refer to this choice of \mathbf{A}_{EXC} as Model I. Meanwhile, \mathbf{A}_{EXC} used in the *standard run* in NSGK (Eq.(31) in [4]) consists of $\mathbf{A}^{(2)}(\Delta\pi)$ and $\mathbf{A}^{(2)}(\Delta\rho)$ alone, and its strength is adjusted to reproduce the $np \rightarrow \gamma d$ rate. We refer to this choice of \mathbf{A}_{EXC} as Model II. For each of Models I and II, Table 3 gives the contributions from the individual terms in A_μ as well as that from V_μ , the vector current. The table indicates that the corrections to the IA values are dominated by the contributions from $\mathbf{A}^{(2)}(\Delta\pi)$ and $\mathbf{A}^{(2)}(\Delta\rho)$.

To facilitate further comparison between Models I and II, we consider the ratio, ξ , defined by $\xi \equiv [\sigma_{\nu d}(\text{IA} + \mathbf{A}_{\text{EXC}}) - \sigma_{\nu d}(\text{IA})]/\sigma_{\nu d}(\text{IA})$. Here, $\sigma_{\nu d}(\text{IA})$ is the result obtained with the IA current alone, while $\sigma_{\nu d}(\text{IA} + \mathbf{A}_{\text{EXC}})$ represents the result obtained with the IA current plus \mathbf{A}_{EXC} . Fig. 1 gives ξ for the CC reaction as a function of E_ν . The solid line shows ξ for Model I, and the dotted line gives ξ for Model II. It is seen that the contribution of \mathbf{A}_{EXC} in Model I is smaller than that in Model II by $2 \sim 4\%$. This difference is mainly due to the reduced strength of the Δ -excitation currents in Model I. For further discussion we normalize $\xi_{(\text{Model II})}$ for the CC reaction by an overall multiplicative factor chosen in such a manner that the normalized $\xi_{(\text{Model II})}$ reproduces $\xi_{(\text{Model I})}$ at the reaction threshold. This normalized result is given by the dash-dotted line in Fig.1. We observe that the dash-dotted line exhibits a slight deviation from the solid line (Model I). This deviation indicates a slight difference of E_ν -dependence between the contribution of \mathbf{A}_{EXC} in Model I and that in Model II. This behavior can be traced to the following facts. (1) Models I and II use somewhat different values of the cut-off parameter, Λ_π , appearing in Eq.(12); $\Lambda_\pi = 0.947$ GeV for Model I, while $\Lambda_\pi = 1.18$ GeV for Model II. (2) The relative strength of $\mathbf{A}^{(2)}(\Delta\pi)$ and $\mathbf{A}^{(2)}(\Delta\rho)$ is different in the two models. The behavior of ξ for the NC reaction (not shown) is similar to ξ for the CC reaction.

The error estimate adopted in NSGK essentially consists in taking the difference between Models I and II as theoretical uncertainty. As mentioned in the introduction, however, Model II, which fails to explain Γ_t^β , should not be given the same status as Model I. To attain a more reasonable estimate of the theoretical uncertainty, we propose the following interpretation of the feature seen in Fig. 1. The fact that Model I has been adjusted to reproduce Γ_t^β means that it can yield model-independent results at a specific kinematics but that, without additional experimental information, the E_ν -dependence of $\sigma_{\nu d}$ cannot be fully controlled. This uncertainty may be assessed from the difference between the solid and dash-dotted lines in Fig.1. From this argument we assign 0.2% uncertainty to the contribution of \mathbf{A}_{EXC} to $\sigma_{\nu d}$ in the solar neutrino energy range, $E_\nu < 20$ MeV.

We recapitulate the discussion regarding the change from $\sigma_{\nu d}(\text{NSGK})$ to $\sigma_{\nu d}(\text{Netal})$: a $\sim 4\%$ enhancement of $\sigma_{\nu d}$ due to the changes in the Fermi constant and g_A and a $\sim 3\%$ reduction due to the use of the new \mathbf{A}_{EXC} (Model I) that reproduces Γ_t^β . These two changes cancel each other to some extent, and the net result is the enhancement of $\sigma_{\nu d}$ by $\sim 1\%$, and this is what is seen in Table 2.

As mentioned earlier, an additional important measure of reliability of our SNPA calculation is obtained by comparing it with the results of an EFT* calculation by Ando *et al.* [24]. By using the value of the low-energy constant, \hat{d}^R , fixed to reproduce the experimental value of Γ_t^β [23], Ando *et al.* [24] have carried out a parameter-free EFT calculation of $\sigma_{\nu d}$. Although the cut-off regularization method used in [24] can introduce the cut-off dependence into the formalism, it has been checked that this dependence is negligibly small for a physically reasonable range of the

cut-off parameter; the relative variation in $\sigma_{\nu d}$ only amounts to 0.02%, which is much smaller than the above-mentioned 0.2% uncertainty inherent in our SNPA calculation. In fact, the uncertainty in $\sigma_{\nu d}$ obtained by Ando *et al.* is dominated by the 0.5% error resulting from the uncertainty in the experimental value of Γ_t^β . We now compare $\sigma_{\nu d}(\text{Netal})$ with $\sigma_{\nu d}(\text{EFT}^*)$ obtained in the EFT* calculation of Ando *et al.* [24] under the same condition regarding the treatment of the radiative corrections. Since Ref.[24] only includes the s-wave of the final NN state, we compare $\sigma_{\nu d}(\text{EFT}^*)$ with $\sigma_{\nu d}(s\text{-wave})$, which represents the s -wave contribution to $\sigma_{\nu d}$ calculated for the *standard case*. The ratio, $\eta \equiv \sigma_{\nu d}(\text{EFT}^*)/\sigma_{\nu d}(s\text{-wave})$, is shown in Table 4, from which we can conclude that SNPA and EFT give identical results at the 1% level.

We proceed to consider the NN potential dependence. As mentioned, the CD-Bonn potential is somewhat distinct from the potentials considered in NSGK, in that it has a significantly smaller D -state probability; $P_D(\text{CD-Bonn}) = 4.2\%$ as compared with $P_D(\text{AV18}) = 5.8\%$. We give in Table 5 the $\sigma_{\nu d}^{NC}$ obtained with the AV18 and CD-Bonn potentials. The difference between the two cases is found to be practically negligible. With the CD-Bonn potential, because of its larger S -state probability, the contribution from the IA current becomes larger, whereas the contribution from \mathbf{A}_{EXC} is smaller due to its reduced D -state probability. Our explicit calculation demonstrates that the cancellation between these two opposing tendencies is almost perfect, providing a yet another manifestation of the robustness of the calculated $\sigma_{\nu d}$. A similar stabilizing mechanism was noticed by Schiavilla *et al.* in their study of the pp -fusion cross section [10].

We now look at R defined by $R \equiv \sigma_{\nu d}^{NC}/\sigma_{\nu d}^{CC}$; R is considered to play an important role in interpreting certain observables in SNO experiments. Table 6 gives the values of R calculated for the various cases discussed above. We can see from the table that R exhibits smaller dependence on the model of the nuclear current (at most 0.5% variation) than $\sigma_{\nu d}^{CC}$ and $\sigma_{\nu d}^{NC}$ themselves. This stability can be understood as follows. We first note the following two features. (1) The contribution of the isoscalar current, which only participates in the NC reaction, is negligibly small in our case; (2) Although the iso-vector vector and axial-vector currents enter in different ways into the nuclear currents responsible for the CC or NC reactions, the contribution of the vector current is much smaller than that of the axial-vector current in the solar neutrino energy regime. As a consequence of these two facts, the transition operators for the NC and CC reactions in the present case are, to good accuracy, related by a rotation in isospin space. So, if there were no isospin breaking effects in the nuclear wave functions, the CC and NC transition amplitudes would be simply related by the Wigner-Eckart theorem in isospin space, leading to the model independence of R . In reality, there are isospin-breaking effects in the two-nucleon wave functions and the final-state phase space, but these “*external effects*” are expected to have little dependence on the model of the nuclear current so long as high-quality NN potentials that reproduce the NN data well are used.

3. Discussion and Summary

Although we do not directly address the issue of radiative corrections (RC) here, we make a few remarks on it. RC can affect $\sigma_{\nu d}$ at the level of a few percents. According to Kurylov *et al.* [17], RC increases $\sigma_{\nu d}^{CC}$ by 4% at low E_ν and by 3% at the higher end of the solar neutrino energy, while RC leads to an E_ν -independent increase of $\sigma_{\nu d}^{NC}$ by $\sim 1.5\%$. The RC for $\sigma_{\nu d}^{CC}$ consists of the “inner” and “outer” corrections. The former is sensitive to hadronic dynamics but energy-independent, while the latter is largely independent of hadronic dynamics but has energy-dependence. Although the results in [17] seem reasonable at the semi-quantitative level, a definitive estimate of RC is yet to be obtained. For instance, we need to examine the relation between RC for the nucleon

and RC for the deuteron. We also need to ascertain whether a proper renormalization procedure has been applied to match the “inner” and “outer” corrections which belong to different energy scales. Until an accurate calculation for RC becomes available, the best one could do is to use the experimental value of G'_F [25] obtained from $0^+ \rightarrow 0^+$ nuclear β -decays instead of G_F obtained from muon decay. This is what we have done in this article. The use of G'_F allows one to take account of the bulk of the “inner” corrections. Along with the use of G'_F , one could use the following procedure to get semi-quantitative estimates of the “outer” corrections. For $\sigma_{\nu d}^{CC}$, take the difference between the result of Kurylov *et al.* (4% - 3%) and the estimated “inner” corrections (2.4%). For $\sigma_{\nu d}^{NC}$ there is no outer corrections at the level of precision of this article.

To summarize, we have improved NSGK’s calculation [4] for the νd reactions by updating some of its inputs and with the use of the axial-vector exchange current the strength of which is controlled by Γ_t^β . We have also taken into account the results of a recent parameter-free EFT calculation [24]. The new value of $\sigma_{\nu d}$, denoted by $\sigma_{\nu d}(\text{Netal})$, is slightly larger than $\sigma_{\nu d}(\text{NSGK})$ reported in [4]; $\sigma_{\nu d}(\text{Netal})/\sigma_{\nu d}(\text{NSGK}) \sim 1.01$. The arguments presented above lead us to conclude that it is reasonable to assign 1% uncertainty to $\sigma_{\nu d}(\text{Netal})$ given in Table 1. The results in Table 1, however, do not include radiative corrections except for those already incorporated into the empirical value of G'_F , which subsumes the bulk of the inner radiative corrections for nuclear β -decay. With the inclusion of the remaining radiative corrections, $\sigma_{\nu d}^{CC}$ is likely to become larger than $\sigma_{\nu d}^{CC}(\text{Netal})$ by up to $\sim 2\%$, while $\sigma_{\nu d}^{NC}$ is expected to lie within the quoted $\sim 1\%$ error of $\sigma_{\nu d}^{NC}(\text{Netal})$.

ACKNOWLEDGMENTS

We are grateful to J. Beacom for his useful criticism on Ref.[4] and for calling our attention to the importance of the radiative corrections. Thanks are also due to R. Machleidt for generously letting us use his computer code for the CD-Bonn potential. This work is supported in part by the US National Science Foundation, Grant No. PHY-9900756 and No. INT-9730847, and also by the Japan Society for the Promotion of Science, Grant No. (c) 12640273.

Appendix: Axial-vector exchange currents

(1) Axial π -exchange Δ -excitation current:

$$\mathbf{A}_{a,ij}^{(2)}(\mathbf{q}; \Delta\pi) = \frac{16}{25} f_A \frac{f_{\pi NN}^2}{m_\pi^2(m_\Delta - m)} \frac{\boldsymbol{\sigma}_j \cdot \mathbf{k}_j}{m_\pi^2 + k_j^2} f_\pi^2(k_j) [4\tau_{j,a} \mathbf{k}_j - (\boldsymbol{\tau}_i \times \boldsymbol{\tau}_j)_a \boldsymbol{\sigma}_i \times \mathbf{k}_j] + (i \rightleftharpoons j). \quad (7)$$

(2) Axial ρ -exchange Δ -excitation current:

$$\begin{aligned} \mathbf{A}_{a,ij}^{(2)}(\mathbf{q}; \Delta\rho) = & -\frac{4}{25} f_A \frac{g_\rho^2(1 + \kappa_\rho)^2}{m^2(m_\Delta - m)} \frac{f_\rho^2(k_j)}{m_\rho^2 + k_j^2} \{4\tau_{j,a} (\boldsymbol{\sigma}_j \times \mathbf{k}_j) \times \mathbf{k}_j - (\boldsymbol{\tau}_i \times \boldsymbol{\tau}_j)_a \boldsymbol{\sigma}_i \times [(\boldsymbol{\sigma}_j \times \mathbf{k}_j) \times \mathbf{k}_j]\} \\ & + (i \rightleftharpoons j). \end{aligned} \quad (8)$$

(3) Axial π -exchange (pair) current:

$$\mathbf{A}_{a,ij}^{(2)}(\mathbf{q}; \pi S) = -\frac{f_A}{m} \frac{f_{\pi NN}^2}{m_\pi^2} \frac{\boldsymbol{\sigma}_j \cdot \mathbf{k}_j}{m_\pi^2 + k_j^2} f_\pi^2(k_j) \{(\boldsymbol{\tau}_i \times \boldsymbol{\tau}_j)_a \boldsymbol{\sigma}_i \times \mathbf{k}_j - \tau_{j,a} [\mathbf{q} + i\boldsymbol{\sigma}_i \times (\mathbf{p}_i + \mathbf{p}'_i)]\} + (i \rightleftharpoons j). \quad (9)$$

(4) Axial ρ -exchange (pair) current:

$$\begin{aligned} \mathbf{A}_{a,ij}^{(2)}(\mathbf{q}; \rho S) = & f_A \frac{g_\rho^2(1 + \kappa_\rho)^2}{4m^3} \frac{f_\rho^2(k_j)}{m_\rho^2 + k_j^2} (\tau_{j,a} \{(\boldsymbol{\sigma}_j \times \mathbf{k}_j) \times \mathbf{k}_j - i[\boldsymbol{\sigma}_i \times (\boldsymbol{\sigma}_j \times \mathbf{k}_j)] \times (\mathbf{p}_i + \mathbf{p}'_i)\} \\ & + (\boldsymbol{\tau}_i \times \boldsymbol{\tau}_j)_a \{q\boldsymbol{\sigma}_i \cdot (\boldsymbol{\sigma}_j \times \mathbf{k}_j) + i(\boldsymbol{\sigma}_j \times \mathbf{k}_j) \times (\mathbf{p}_i + \mathbf{p}'_i) - [\boldsymbol{\sigma}_i \times (\boldsymbol{\sigma}_j \times \mathbf{k}_j)] \times \mathbf{k}_j\}) + (i \rightleftharpoons j). \end{aligned} \quad (10)$$

(5) Axial $\pi\rho$ current:

$$\mathbf{A}_{a,ij}^{(2)}(\mathbf{q}; \pi\rho) = 2f_A \frac{g_\rho^2}{m} \frac{\boldsymbol{\sigma}_j \cdot \mathbf{k}_j}{(m_\rho^2 + k_i^2)(m_\pi^2 + k_j^2)} f_\rho(k_i) f_\pi(k_j) (\boldsymbol{\tau}_i \times \boldsymbol{\tau}_j)_a [(1 + \kappa_\rho) \boldsymbol{\sigma}_i \times \mathbf{k}_i - i(\mathbf{p}_i + \mathbf{p}'_i)] + (i \rightleftharpoons j). \quad (11)$$

Here a indicates the a -th isospin component; m_π , m_ρ , m , and m_Δ are the masses of the pion, ρ -meson, nucleon and Δ -particle, respectively. f_A is the axial form factor given in Eq.(1). We have also introduced the total momentum transfer, $\mathbf{q} \equiv \mathbf{k}_i + \mathbf{k}_j$, with $\mathbf{k}_{i(j)}$ being the momentum transferred to the i -th (j -th) nucleon; \mathbf{p}_i and \mathbf{p}'_i are the initial and final momenta of the i -th nucleon. The form factor, $f_{\pi(\rho)}(k)$, for the pion-nucleon (ρ -nucleon) vertex is parametrized as

$$f_{\pi(\rho)}(k) = \frac{\Lambda_{\pi(\rho)}^2 - m_\pi^2}{\Lambda_{\pi(\rho)}^2 + \mathbf{k}^2}, \quad (12)$$

with $\Lambda_\pi = 4.8 \text{ fm}^{-1}$ and $\Lambda_\rho = 6.8 \text{ fm}^{-1}$. The quark model has been used to relate the $\pi N\Delta$, $\rho N\Delta$ and $A_\mu N\Delta$ couplings to the πNN , ρNN , and $A_\mu NN$ couplings, respectively. As pointed out in [10], reducing the quark-model value for the $A_\mu N\Delta$ coupling in $\mathbf{A}^{(2)}(\Delta\pi)$ and $\mathbf{A}^{(2)}(\Delta\rho)$ by 20% brings the theoretical and experiment values of Γ_t^β into agreement. In our calculation, therefore, we use $\mathbf{A}^{(2)}(\Delta\pi)$ in Eq.(7) and $\mathbf{A}^{(2)}(\Delta\rho)$ in Eq.(8), each with a factor of 0.8 multiplied.

References

- [1] The SNO Collaboration, Phys. Lett. B 194 (1987) 321, and references therein.
- [2] Q. Ahmad *et al.*, Phys. Rev. Lett. 87 (2001) 071301.
- [3] N. Tataru, Y. Kohyama and K. Kubodera, Phys. Rev. C 42 (1990) 1694; S. Ying, W. C. Haxton and E. M. Henley, Phys. Rev. C 45 (1992) 1982; for a review, see K. Kubodera and S. Nozawa, Int. J. Mod. Phys. E 3 (1994) 101.
- [4] S. Nakamura, T. Sato, V. Gudkov and K. Kubodera, Phys. Rev. C 63 (2001) 034617.
- [5] M. Butler and J.-W. Chen, Nucl. Phys. A675 (2000) 575; M. Butler, J.-W. Chen and X. Kong, Phys. Rev. C 63 (2001) 035501.
- [6] S. Fukuda *et al.*, Phys. Rev. Lett. 86 (2001) 5651.
- [7] M. Chemtob and M. Rho, Nucl. Phys. A163 (1971) 1.
- [8] For a recent review, see J. Carlson and R. Schiavilla, Rev. Mod. Phys. 70 (1998) 743.
- [9] J. Carlson, D. O. Riska, R. Schiavilla and R. B. Wiringa, Phys. Rev. C 44 (1991) 619.
- [10] R. Schiavilla, V. G. J. Stoks, W. Glöckle, H. Kamada, A. Nogga, J. Carlson, R. Machleidt, V. R. Pandharipande, R. B. Wiringa, A. Kievsky, S. Rosati and M. Viviani, Phys. Rev. C 58 (1998) 1263.
- [11] S. Weinberg, Phys. Lett. B 251 288 (1990); Nucl. Phys. B363 (1991) 3.
- [12] E. Epelbaum, W. Glöckle and U.-G. Meißner, Nucl. Phys. A671 295 (2000); E. Epelbaum, H. Kamada, A. Nogga, H. Witaa, W. Glöckle, Ulf-G. Meißner, Phys. Rev. Lett. 86 (2001) 4787.

- [13] For a review, see U. van Kolck, Prog. Part. Nucl. 43 (1999) 337; S.R. Beane *et al.*, in: At the Frontiers of Particle Physics - Handbook of QCD, Vol. 1, eds. M. Shifman, (World Scientific, Singapore, 2001).
- [14] D. B. Kaplan, M. J. Savage and M. B. Wise, Nucl. Phys. B478 (1996) 629; Phys. Lett. B 424 (1998) 390.
- [15] J. F. Beacom and S. J. Parke, Phys. Rev. D 64 (2001) 091302; J. F. Beacom, private communication.
- [16] I. S. Towner, Phys. Rev. C 58 (1998) 1288.
- [17] A. Kurylov, M. J. Ramsey-Musolf and P. Vogel, nucl-th/0110051.
- [18] R. B. Wiringa, V. G. J. Stoks and R. Schiavilla, Phys. Rev. C 51 (1995) 38.
- [19] V. G. J. Stoks, R. A. M. Klomp, C. P. F. Terheggen and J. J. de Swart, Phys. Rev. C 49 (1994) 2950.
- [20] R. Machleidt, Phys. Rev. C 63 (2001) 024001.
- [21] T.-S. Park, D.-P. Min and M. Rho, Phys. Rev. Lett. 74 (1995) 4153.
- [22] T.-S. Park, K. Kubodera, D.-P. Min and M. Rho, Nucl. Phys. A684 (2001) 101, and references therein.
- [23] T.-S. Park, L. E. Marcucci, R. Schiavilla, M. Viviani, A. Kievsky, S. Rosati, K. Kubodera, D.-P. Min and M. Rho, nucl-th/0106025; nucl-th/0107012.
- [24] S. Ando *et al.*, in preparation.
- [25] I. S. Towner and J. C. Hardy, in: Physics beyond the standard model, eds. P. Herczeg, C.M. Hoffman and H.V. Klapdor-Kleingrothaus, (World Scientific, Singapore, 1999) p. 338.
- [26] V. Bernard, L. Elouadrhiri and U.-G. Meißner, hep-ph/0107088.

Figure 1: Contributions of \mathbf{A}_{EXC} to $\sigma_{\nu d}^{CC}$; ξ defined in the text is plotted for Model I (solid line) and Model II (dashed line). The dash-dotted line represents the “normalized” version of Model II described in the text.

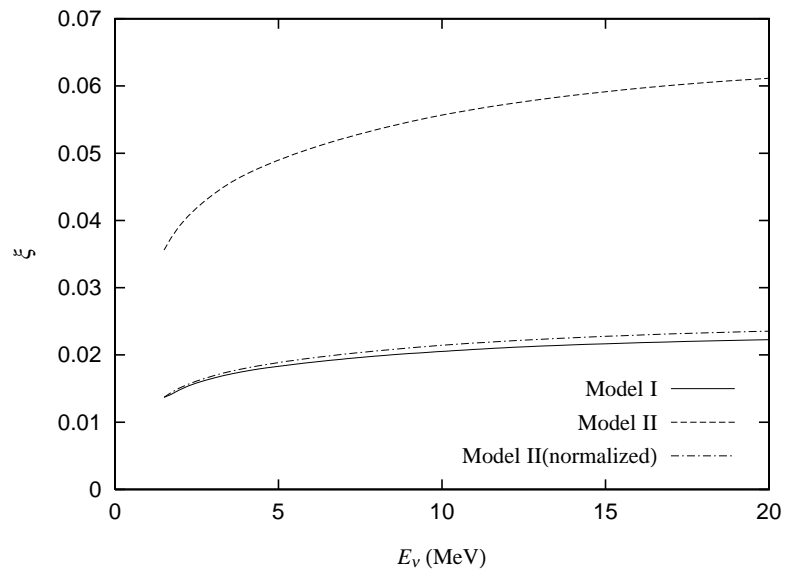


Table 1: Calculated values of $\sigma_{\nu d}^{CC}$ and $\sigma_{\nu d}^{NC}$ in units of cm^2 . The “- x ” in the parentheses means 10^{-x} ; thus an entry like 4.579(-48) stands for $4.579 \times 10^{-48} \text{ cm}^2$.

E_ν (MeV)	$\nu_e d \rightarrow e^- pp$	$\nu d \rightarrow \nu pn$	E_ν (MeV)	$\nu_e d \rightarrow e^- pp$	$\nu d \rightarrow \nu pn$
1.5	4.680 (-48)	0.000 (0)	8.8	1.911 (-42)	7.530 (-43)
1.6	1.147 (-46)	0.000 (0)	9.0	2.034 (-42)	8.070 (-43)
1.8	1.147 (-45)	0.000 (0)	9.2	2.160 (-42)	8.629 (-43)
2.0	3.670 (-45)	0.000 (0)	9.4	2.291 (-42)	9.209 (-43)
2.2	7.973 (-45)	0.000 (0)	9.6	2.425 (-42)	9.809 (-43)
2.4	1.428 (-44)	4.346 (-47)	9.8	2.565 (-42)	1.043 (-42)
2.6	2.279 (-44)	4.322 (-46)	10.0	2.708 (-42)	1.107 (-42)
2.8	3.369 (-44)	1.478 (-45)	10.2	2.856 (-42)	1.173 (-42)
3.0	4.712 (-44)	3.402 (-45)	10.4	3.007 (-42)	1.241 (-42)
3.2	6.324 (-44)	6.372 (-45)	10.6	3.164 (-42)	1.311 (-42)
3.4	8.216 (-44)	1.052 (-44)	10.8	3.324 (-42)	1.383 (-42)
3.6	1.040 (-43)	1.594 (-44)	11.0	3.489 (-42)	1.458 (-42)
3.8	1.289 (-43)	2.274 (-44)	11.2	3.658 (-42)	1.534 (-42)
4.0	1.569 (-43)	3.098 (-44)	11.4	3.832 (-42)	1.612 (-42)
4.2	1.881 (-43)	4.072 (-44)	11.6	4.010 (-42)	1.693 (-42)
4.4	2.225 (-43)	5.202 (-44)	11.8	4.192 (-42)	1.775 (-42)
4.6	2.604 (-43)	6.492 (-44)	12.0	4.379 (-42)	1.860 (-42)
4.8	3.016 (-43)	7.947 (-44)	12.2	4.570 (-42)	1.947 (-42)
5.0	3.463 (-43)	9.570 (-44)	12.4	4.766 (-42)	2.035 (-42)
5.2	3.945 (-43)	1.136 (-43)	12.6	4.966 (-42)	2.126 (-42)
5.4	4.463 (-43)	1.333 (-43)	12.8	5.171 (-42)	2.219 (-42)
5.6	5.017 (-43)	1.548 (-43)	13.0	5.380 (-42)	2.314 (-42)
5.8	5.608 (-43)	1.780 (-43)	13.5	5.923 (-42)	2.561 (-42)
6.0	6.236 (-43)	2.031 (-43)	14.0	6.495 (-42)	2.822 (-42)
6.2	6.902 (-43)	2.300 (-43)	14.5	7.095 (-42)	3.095 (-42)
6.4	7.605 (-43)	2.587 (-43)	15.0	7.724 (-42)	3.382 (-42)
6.6	8.347 (-43)	2.894 (-43)	15.5	8.383 (-42)	3.682 (-42)
6.8	9.127 (-43)	3.219 (-43)	16.0	9.071 (-42)	3.995 (-42)
7.0	9.946 (-43)	3.562 (-43)	16.5	9.789 (-42)	4.323 (-42)
7.2	1.080 (-42)	3.925 (-43)	17.0	1.054 (-41)	4.663 (-42)
7.4	1.170 (-42)	4.308 (-43)	17.5	1.131 (-41)	5.017 (-42)
7.6	1.264 (-42)	4.709 (-43)	18.0	1.212 (-41)	5.385 (-42)
7.8	1.362 (-42)	5.130 (-43)	18.5	1.296 (-41)	5.767 (-42)
8.0	1.464 (-42)	5.571 (-43)	19.0	1.383 (-41)	6.162 (-42)
8.2	1.569 (-42)	6.031 (-43)	19.5	1.474 (-41)	6.571 (-42)
8.4	1.679 (-42)	6.511 (-43)	20.0	1.567 (-41)	6.994 (-42)
8.6	1.793 (-42)	7.010 (-43)			

Table 2: Comparison of the present results with those of NSGK [4]. The ratio, $\sigma_{\nu d}(\text{Netal})/\sigma_{\nu d}(\text{NSGK})$, is given for representative values of E_ν .

E_ν (MeV)	$\nu_e d \rightarrow e^- pp$	$\nu d \rightarrow \nu pn$
5	1.013	1.011
10	1.008	1.006
15	1.006	1.003
20	1.004	1.001

Table 3: For Models I and II are shown the cumulative contributions to $\sigma_{\nu d}^{CC}$ from the various components in the current. The row labeled “IA” gives $\sigma_{\nu d}^{CC}$ obtained with the IA currents in A_μ and V_μ , and the next row labeled “+ \mathbf{V}_{EXC} ” gives $\sigma_{\nu d}^{CC}$ that includes the contributions of the IA currents and \mathbf{V}_{EXC} , the exchange current in \mathbf{V} . Similarly, an entry in the n -th row (counting from the row labeled “IA”) includes the coherent contributions of all the currents listed in the first n rows. The numbers in the last row are obtained with the full currents. The parenthesized number in the n -th row gives the ratio, $\sigma_{\nu d}^{CC}(n\text{-th row})/\sigma_{\nu d}^{CC}((n-1)\text{-th row})$, which represents a factor by which $\sigma_{\nu d}^{CC}$ changes when the new term is added.

$\sigma_{\nu d}^{CC} (\times 10^{-42} \text{cm}^2)$				
Model I				
E_ν	5 MeV	10 MeV	15 MeV	20 MeV
IA	0.3397 (-)	2.646 (-)	7.526 (-)	15.23 (-)
+ \mathbf{V}_{EXC}	0.3401 (1.001)	2.654 (1.003)	7.560 (1.005)	15.33 (1.006)
+ $\pi\Delta$	0.3474 (1.022)	2.719 (1.025)	7.758 (1.026)	15.74 (1.027)
+ $\rho\Delta$	0.3448 (0.992)	2.695 (0.991)	7.687 (0.991)	15.59 (0.991)
+ πS	0.3456 (1.002)	2.702 (1.003)	7.707 (1.003)	15.63 (1.003)
+ ρS	0.3447 (0.997)	2.694 (0.997)	7.682 (0.997)	15.58 (0.997)
+ $\pi - \rho$	0.3463 (1.005)	2.708 (1.005)	7.724 (1.005)	15.67 (1.006)
+ A_{EXC}^0	0.3463 (1.000)	2.708 (1.000)	7.724 (1.000)	15.67 (1.000)
Model II				
E_ν	5 MeV	10 MeV	15 MeV	20 MeV
IA	0.3397 (-)	2.646 (-)	7.526 (-)	15.23 (-)
+ \mathbf{V}_{EXC}	0.3401 (1.001)	2.654 (1.003)	7.560 (1.005)	15.33 (1.006)
+ $\pi\Delta$	0.3612 (1.062)	2.841 (1.071)	8.128 (1.075)	16.52 (1.078)
+ $\rho\Delta$	0.3567 (0.988)	2.801 (0.986)	8.007 (0.985)	16.26 (0.985)
+ A_{EXC}^0	0.3567 (1.000)	2.801 (1.000)	8.008 (1.000)	16.26 (1.000)

Table 4: Comparison of SNPA and EFT calculations. The ratio, $\eta \equiv \sigma_{\nu d}(\text{EFT}^*)/\sigma_{\nu d}(s\text{-wave})$, is given for representative values of E_ν .

E_ν (MeV)	$\nu_e d \rightarrow e^- pp$	$\nu d \rightarrow \nu pn$
5	1.003	1.004
10	1.001	1.003
15	0.999	1.002
20	0.998	1.001

Table 5: Dependence of $\sigma_{\nu d}^{NC}$ on NN potentials. ‘Bonn’ and ‘AV18’ represent the results obtained with the CD-Bonn and the AV18 potentials, respectively.

E_ν	$\sigma_{\nu d}^{NC} (\times 10^{-42} \text{cm}^2)$							
	5 MeV		10 MeV		15 MeV		20 MeV	
	Bonn	AV18	Bonn	AV18	Bonn	AV18	Bonn	AV18
IA	0.09459	0.09390	1.091	1.083	3.327	3.300	6.871	6.814
IA+EXC	0.09557	0.09570	1.104	1.107	3.373	3.382	6.973	6.994

Table 6: The ratio, $R \equiv \sigma(\nu d \rightarrow \nu np)/\sigma(\nu_e d \rightarrow e^- pp)$, calculated for representative values of E_ν . The second column gives R_{std} corresponding to the *standard case*. The third and fourth columns give R_{IA}/R_{std} and $R_{[\text{Model II}]} / R_{std}$, respectively. Here R_{IA} corresponds to R obtained with the IA current alone, while $R_{[\text{Model II}]}$ corresponds to Model II.

E_ν (MeV)	R_{std}	IA	Model II
5	0.2764	1.000	1.004
10	0.4087	1.001	1.004
15	0.4378	1.002	1.004
20	0.4464	1.002	1.005